available at www.sciencedirect.com

ScienceDirect

journal homepage: www.elsevier.com/locate/biochempharm

The changes of intracellular H_2O_2 are an important factor maintaining mitochondria membrane potential of antimycin A-treated As4.1 juxtaglomerular cells

Yong Whan Han, Sung Zoo Kim, Suhn Hee Kim, Woo Hyun Park *

Department of Physiology, Medical School, Institute for Medical Sciences, Center for Healthcare Technology Development, Chonbuk National University, JeonJu 561-180, Republic of Korea

ARTICLE INFO

Article history:
Received 21 September 2006
Accepted 21 November 2006

Keywords:
Antimycin A
ROS
Cell cycle
Apoptosis
As4.1
ROS scavenger
SOD
Catalase

ABSTRACT

We investigated an involvement of ROS, such as H_2O_2 and $O_2^{\bullet-}$ and GSH in the As4.1 cell death by antimycin A and examined whether ROS scavengers rescue antimycin A-induced As4.1 cell death and its mechanism. Levels of intracellular H_2O_2 and $O_2^{\bullet-}$ were markedly increased in antimycin A-treated cells. Antimycin A reduced the intracellular GSH content. A ROS scavenger, Tiron down-regulated the production of intracellular H_2O_2. However, the reduction of intracellular H_2O_2 level did not change the apoptosis parameters, such as sub-G1 DNA content and annexin V binding. Interestingly, treatment of Tiron could partially prevent the loss of mitochondrial transmembrane potential ($\Delta\Psi_m$). Treatment of SOD and catalase also reduced the intracellular H_2O_2 and loss of mitochondrial transmembrane potential ($\Delta\Psi_m$) without reducing $O_2^{\bullet-}$ level and apoptosis in antimycin A-treated As4.1 cells. All the ROS scavengers, SOD and catalase did not inhibit GSH depletion induced by antimycin A, resulting in failure of preventing the apoptosis. In addition, all the reagents including antimycin A did not induce any specific phase arrest of cell cycle in As4.1 cells. In summary, these results demonstrate that antimycin A generates potently ROS, H_2O_2 and $O_2^{\bullet-}$ and induces the depletion of GSH content in As4.1 JG cells, and that Tiron, SOD and catalase inhibited partially the loss of mitochondrial transmembrane potential ($\Delta\Psi_m$) via the reduction of intracellular H_2O_2 level.

1. Introduction

Reactive oxygen species (ROS) include hydrogen peroxide (H_2O_2), nitric oxide (NO), superoxide anion ($O_2^{\bullet-}$), hydroxyl radical ($^{\bullet}OH$) and peroxynitrite ($ONOO^-$). ROS have recently been implicated in the regulation of various important cellular events, including transcription factor activation, gene expression, differentiation and cell proliferation [1–3]. ROS are formed as byproducts of mitochondrial respiration or precise oxidases including nicotine adenine diphosphate (NADPH) oxidase, xanthine oxidase (XO) and certain arachidonic acid oxygenases [4]. An alteration on the redox state of the tissue implies a change in ROS generation or metabolism. Principal metabolic pathway involves superoxide dismutase

* *Corresponding author*. Tel.: +82 63 270 3079; fax: +82 63 274 9892.
E-mail address: parkwh71@chonbuk.ac.kr (W.H. Park).

Abbreviations: AMA, antimycin A; ROS, reactive oxygen species; NADPH, nicotine adenine diphosphate; XO, xanthine oxidase; SOD, superoxide dismutase; JGCT, juxtaglomerular cell tumors; FBS, fetal bovine serum; PBS, phosphate buffer saline; FITC, fluorescein isothiocyanate; H_2DCFDA, 2′,7′-dichlorodihydrofluorescein diacetate; DHE, dihydroethidium; GSH, glutathione; NAC, *N*-acetylcysteine; CMFDA, 5-chloromethylfluorescein diacetate

0006-2952/$ – see front matter
doi:10.1016/j.bcp.2006.11.017

(SOD), which is expressed as extracellular, intracellular and mitochondrial isoforms, and metabolizes $O_2^{\bullet-}$ to H_2O_2. Further metabolism by peroxidases that include catalase and glutathione peroxidase yields O_2 and H_2O [5]. Cells possess antioxidant systems to control the redox state, which is important for their survival. Excessive production of ROS gives rise to activation of events, which lead to death and survival in several types of cells [6–9]. The precise mechanisms involved in cell death induced by ROS remain an open question and the protective effect of some antioxidants on cell death is still controversial.

Antimycin A (AMA) is a mixture product of predominantly antimycin A1 and A3 derived from *Streptomyces kitazawensis* [10]. The compound inhibits the activity of succinate oxidase and NADH oxidase and also blocks mitochondrial electron transport specifically between cytochromes *b* and *c* [11–14]. Inhibition of electron transport causes a collapse of the proton gradient across the mitochondrial inner membrane, thereby collapsing the mitochondrial membrane potential ($\Delta\Psi_m$) [11,13,15]. This inhibition also causes the production of ROS [15,16]. There is evidence that either ROS or the collapse of mitochondrial membrane potential ($\Delta\Psi_m$) opens the mitochondrial permeability transition pore, accompanied by the release of proapoptotic molecules, such as cytochrome *c* into the cytoplasm [17–19]. In fact, because AMA acts directly on the mitochondria, AMA-induced apoptosis has been reported in many experiments [20–23].

Juxtaglomerular cell tumors (JGCTs; also known as reninomas), first described in the late 1960s [24,25], are rare benign tumors of the kidney. About 100 cases have been described to date. Reninomas are understood to arise from juxtaglomerular cells. Clinically, the patients suffer from headaches, polyuria, nocturia and dizziness including other symptoms. Hypertension is a sign in almost all patients and laboratory findings of hyperreninemia, hyperaldosteronism and hypokalemia are characteristic. Recently, a malignant JGCT was described [26].

As4.1 cells have been used as a model for the JG cell. This cell line was isolated from kidney neoplasm in a transgenic mouse containing a renin SV40 T-antigen transgene [27]. However, the role of ROS in kidney cell death, especially JG cell, has not been evaluated. Therefore, understanding the molecular mechanism of kidney cell death by ROS generator, especially AMA is an important subject. In the present study, we evaluated the involvement of ROS, such as H_2O_2 and $O_2^{\bullet-}$ and GSH in the AMA-treated As4.1 cells and investigated whether ROS scavengers could rescue AMA-induced As4.1 cell death and its mechanism.

2. Materials and methods

2.1. Cell culture

As4.1 cells (ATCC No. CRL-2193) are a renin-expressing clonal cell line derived from the kidney neoplasm of a transgenic mouse [27]. As4.1 cells were cultured in DMEM supplemented with 10% fetal bovine serum (FBS) and 1% penicillin–streptomycin (GIBCO BRL, Grand Island, NY). Cell cultures were maintained in a humidified incubator containing 5% CO_2 at 37 °C. Cells were routinely grown in 100-mm plastic tissue culture dish (Nunc, Roskilde, Denmark) and were passed when they were in logarithmic phase of growth, and maintained at the above-described culture conditions for all experiments.

2.2. Reagents

AMA (Sigma–Aldrich Chemical Company, St. Louis, MO) was dissolved in ethanol at 2×10^{-2} M as a stock solution. The cell permeable $O_2^{\bullet-}$ scavengers, 4-hydroxy-TEMPO (4-hydroxyl-2,2,6,6-tetramethylpierydine-1-oxyl) (Tempol), (4,5-dihydroxyl-1,3-benzededisulfonic acid) (Tiron), (1-[2,3,4-trimethoxibenzyl]-piperazine) (Trimetazidine) and (*N*-acetylcysteine) (NAC) were obtained from Sigma. These were dissolved in designated solution buffer at 1×10^{-1} M as a stock solution. All of stock solutions wrapped in foil were kept in 4 or −20 °C.

2.3. Cell cycle and sub-G_1 analysis

Cell cycle and sub-G_1 distribution were determined by staining DNA with propidium iodide (PI; Sigma–Aldrich) as described used [28]. Briefly, 1×10^6 cells were incubated with the designated doses of AMA with or without ROS scavenger, SOD or catalase for 48–72 h. Cells were then washed with phosphate buffer saline (PBS) and fixed in 70% ethanol. Cells were again washed with PBS and then incubated with PI (10 μg) with simultaneous treatment of RNase at 37 °C for 30 min. The percentages of cells in the different phases of the cell cycle or having the sub-G_1 DNA content were measured with FACStar flow cytometer (Becton Dickinson, San Jose, CA) and analyzed using lysis II and cellfit software (Becton Dickinson) or ModFit software (Verity Software Inc.).

2.4. Annexin V/PI staining

Apoptosis was determined by staining cells with annexin V-fluorescein isothiocyanate (FITC) or -phycoerythrin (PE) and PI labeling. Annexin V was used to detect early apoptotic cells during apoptosis. Briefly, to quantitate the apoptosis of cells, 1×10^6 cells were incubated with the designated doses of AMA with or without ROS scavenger, SOD or catalase for 48–72 h. The cells were washed twice with cold PBS, and suspended in 500 μl of binding buffer (10 mM HEPES/NaOH [pH 7.4], 140 mM NaCl, 2.5 mM $CaCl_2$) at a concentration of 1×10^6 cells/ml. Then 5 μl of annexin V-FITC or -PE (PharMingen, San Diego, CA) and PI (1 μg/ml) were added to these cells at 37 °C for 30 min. The cells were analyzed with FACStar flow cytometer (Becton Dickinson). Viable cells were negative for both PI and annexin V, and apoptotic cells were positive for annexin V and negative for PI, whereas late apoptotic dead cells displayed both high annexin V and PI labeling. Non-viable cells, which underwent necrosis, were positive for PI and negative for annexin V.

2.5. Measurement of mitochondrial membrane potential ($\Delta\Psi_m$)

Mitochondrial membrane was monitored using a cell permeable cationic, fluorescent dye Rhodamine 123, which preferentially enters into mitochondria due to the highly negative

mitochondrial membrane potential ($\Delta\Psi_m$). Depolarization of mitochondrial membrane potential ($\Delta\Psi_m$) results in the loss of Rhodamine 123 from the mitochondria thereby decreasing intracellular fluorescence. Briefly, 1×10^6 cells were incubated with the designated doses of AMA with or without ROS scavenger, SOD or catalase for 48–72 h. The cells were washed twice with PBS and incubated with Rhodamine 123 (0.1 μg/ml; Sigma) at 37 °C for 30 min. Subsequently, PI (1 μg/ml) was added, and Rhodamine 123 and PI staining intensity were determined by flow cytometry.

2.6. Detection of intracellular H_2O_2 and $O_2^{\bullet-}$ concentration

Intracellular H_2O_2 concentration was detected by means of an oxidation-sensitive fluorescent probe dye, 2′,7′-dichlorodihydrofluorescein diacetate (H_2DCFDA) (Invitrogen Molecular Probes, Eugene, OR). H_2DCFDA was deacetylated intracellularly by non-specific esterase, which was further oxidized by cellular peroxides to the fluorescent compound 2,7-dichlorofluorescein (DCF). Dihydroethidium (DHE) (Invitrogen Molecular Probes) is a fluorogenic probe that is highly selective for superoxide anion radical detection. DHE is cell permeable and reacts with superoxide anion to form ethidium, which in turn intercalates in the deoxyribonucleic acid, thereby exhibiting a red fluorescence. Briefly, cells were incubated with the designated doses of AMA with or without ROS scavenger, SOD or catalase for 48–72 h. The cells were then washed with PBS. They were then incubated with 20 μM H_2DCFDA or 5 μM DHE at 37 °C for 30 min according to the manufacturer's instructions. DCF fluorescence and Red fluorescence were detected by FACStar flow cytometer (Becton Dickinson). For each sample, 5000 or 10,000 events were collected. H_2O_2 and $O_2^{\bullet-}$ production were expressed as mean fluorescence intensity (MFI), which was calculated by CellQuest software.

2.7. Detection of intracellular glutathione (GSH)

Cellular GSH levels were analyzed using 5-chloromethylfluorescein diacetate (CMFDA, Molecular Probes). It is a useful membrane-permeable dye for determining levels of intracellular glutathione [29–31]. Briefly, cells were incubated with the designated doses of AMA with or without ROS scavenger, SOD or catalase for 48–72 h. The cells were then washed in PBS. They were then incubated with 5 μM CMFDA at 37 °C for 30 min according to the manufacturer's instructions. Cytoplasmic esterases convert non-fluorescent CMFDA to fluorescent 5-chloromethylfluorescein, which can then react with the glutathione. CMF fluorescence was detected by FACStar flow cytometer (Becton Dickinson), which was calculated by CellQuest software. For each sample, 5000 or 10,000 events were collected.

2.8. Statistical analysis

Results represent the mean of at least two or three independent experiments; bar, S.E.M. Statistical analysis was performed using student's *t*-test to evaluate differences between the groups. The software for Microsoft Excel was used for this analysis. Statistical significance was defined as $p < 0.05$.

3. Results

3.1. Effect of AMA on ROS and GSH production in As4.1 cells

To assess the production of intracellular H_2O_2 in the AMA-treated As4.1 cells, we used H_2DCFDA fluorescence dye. As shown in Fig. 1A and B, intracellular H_2O_2 levels were

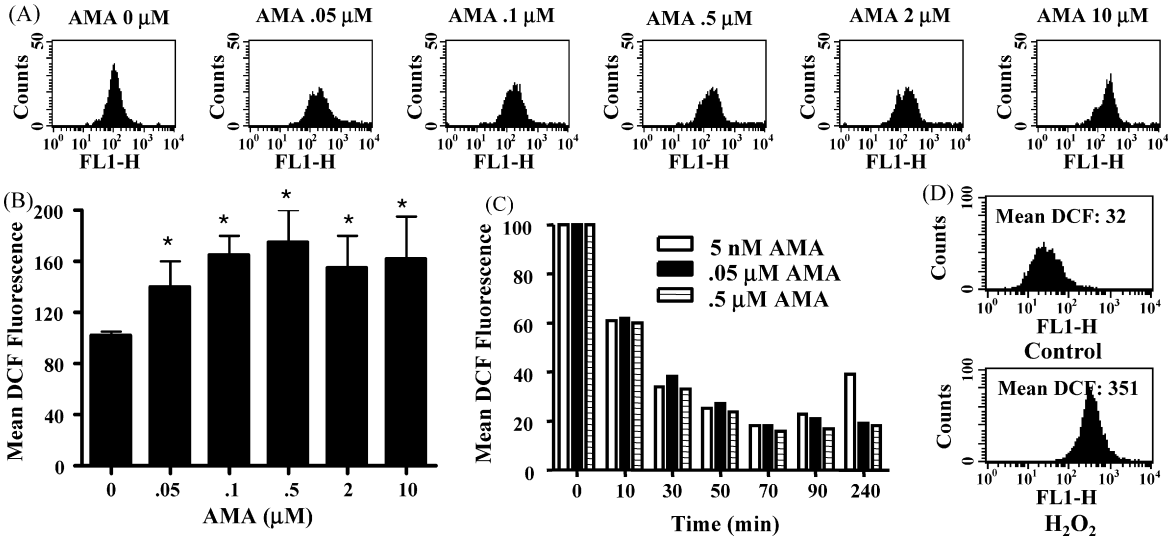

Fig. 1 – Effects of AMA on ROS production, H_2O_2 in As4.1 cells. (A) Exponentially growing cells were treated with the indicated AMA for 48 h. Intracellular H_2O_2 level was determined by FACStar flow cytometer as described in Section 2. (B) Graph shows the levels of mean DCF fluorescence of A. (C) Graph shows the intracellular H_2O_2 level for the designated concentration and times. (D) The increased levels of mean DCF fluorescence in 100 mM H_2O_2-treated cells. $^*p < 0.05$ compared with the control group.

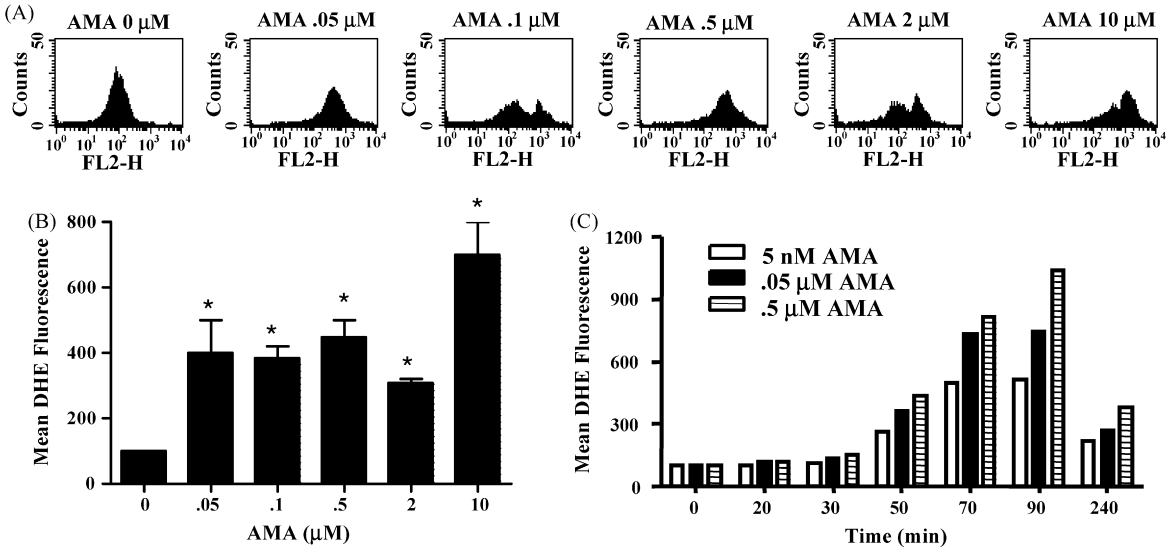

Fig. 2 – Effects of AMA on ROS production, $O_2^{\bullet-}$ in As4.1 cells. (A) Exponentially growing cells were treated with the indicated AMA for 48 h. Intracellular $O_2^{\bullet-}$ level was determined by FACStar flow cytometer as described in Section 2. (B) Graph shows the levels of mean DHE fluorescence of A. (C) Graph shows the intracellular $O_2^{\bullet-}$ level for the designated concentration and times. $^*p < 0.05$ compared with the control group.

significantly increased in As4.1 cells treated with AMA for 48 h. However, the decreased pattern of H_2O_2 levels by this drug (5 nM, 0.05 and 0.5 μM) was clearly detected within 10 min (Fig. 1C). Then, a slow increase of H_2O_2 levels by 5 nM AMA was observed after about 90 min. As shown in Fig. 1D, our method to detect the production of intracellular H_2O_2 using the H_2DCFDA fluorescence was likely to be correct, since we could obviously observe the increasing DCF fluorescence in the H_2O_2-treated As4.1 cells in our experimental condition.

Next, we determined the change of intracellular $O_2^{\bullet-}$ in the AMA-treated As4.1 cells. Red fluorescence derived from DHE, reflecting $O_2^{\bullet-}$ accumulation, was significantly increased approximately five times in As4.1 cells treated with AMA compared to that of the control cells (Fig. 2A and B). The accumulation of $O_2^{\bullet-}$ was observed at the early time (50 min) in a dose dependent manner of AMA (Fig. 2C). Maximum generation of $O_2^{\bullet-}$ was reached at about 90 min after treatment of 0.5 μM AMA was and was approximately 10 times higher than that of the control cells. The level was then decreased after about 90 min.

Cellular GSH has been shown to be crucial for regulation of cell proliferation, cell cycle progression and apoptosis [32,33]. We therefore analyzed the changes of GSH level in As4.1 cells by using CMF fluorescence. The M1 population of As4.1 cells showed lower level of intracellular GSH content. AMA significantly elevated the percentages of cells residing in the M1 population in a dose-dependent manner at the 48 h (Fig. 3), indicating the depletion of intracellular GSH content in As4.1 cells by AMA. The critical depletion changes of intracellular GSH content were observed at less than 0.05 μM concentration of AMA. The decrease of intracellular GSH content was observed in the early time of 20 min on the exposure to 5 nM, 0.05 and 0.5 μM of AMA (data not shown).

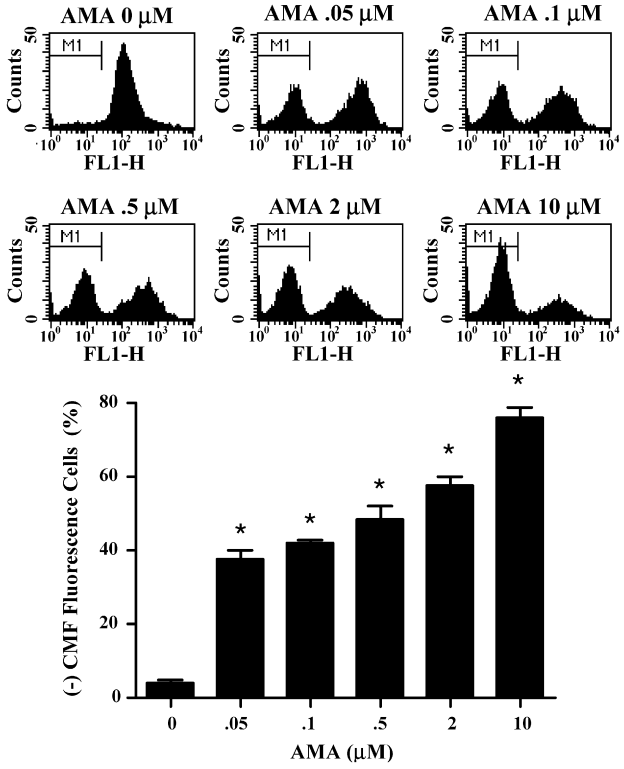

Fig. 3 – Effects of AMA on GSH production in As4.1 cells. Exponentially growing cells were treated with the indicated AMA for 48 h. Intracellular GSH level was determined by FACStar flow cytometer as described in Section 2. Graph shows the levels of mean CMF fluorescence of above figures. $^*p < 0.05$ compared with the control group.

3.2. *Effects of ROS scavengers on ROS production, GSH depletion and apoptosis in AMA-treated As4.1 cells*

To determine whether ROS production and GSH depletion in AMA-treated As4.1 cells are changed by ROS scavengers, cell-permeable ROS scavenger, Tempol or Tiron [34], or a well-known antioxidant, NAC were co-incubated with the AMA-treated As4.1 cells for 48 h. Also an anti-ischemic and metabolic agent, Trimetazidine was used as an indirect antioxidant [35,36]. To measure the accurate intracellular fluorescence level of ROS, we used only the cells residing in the R2 region, which could be considered cells with intact plasma membrane (Fig. 4A and B). As shown in Fig. 4A and D, the increased level of H_2O_2 by 0.05 μM AMA was not significantly decreased by Tempol (50 μM), Trimetazidine (50 μM) or NAC (50 μM). However, treatment of Tiron decreased the level of H_2O_2 in As4.1 cells treated with 0.05 μM AMA below the level of control cells. In regard to the $O_2^{\bullet-}$ levels by these ROS scavengers, Tempol and Trimetazidine slightly augmented the $O_2^{\bullet-}$ levels in AMA-treated cells instead (Fig. 4B and E). Tiron did not alter the $O_2^{\bullet-}$ levels. Interestingly, NAC (50 μM) significantly enhanced the $O_2^{\bullet-}$ levels in AMA-treated cells (Fig. 4B and E). In addition, the scavengers did not decrease the depletion of GSH content in As4.1 cells treated with AMA (Fig. 4C and F). Only NAC intensified the depletion of GSH content in AMA-treated cells (Fig. 4C and F).

We also examined whether ROS scavengers prevent AMA-induced As4.1 cell death. All the scavengers could

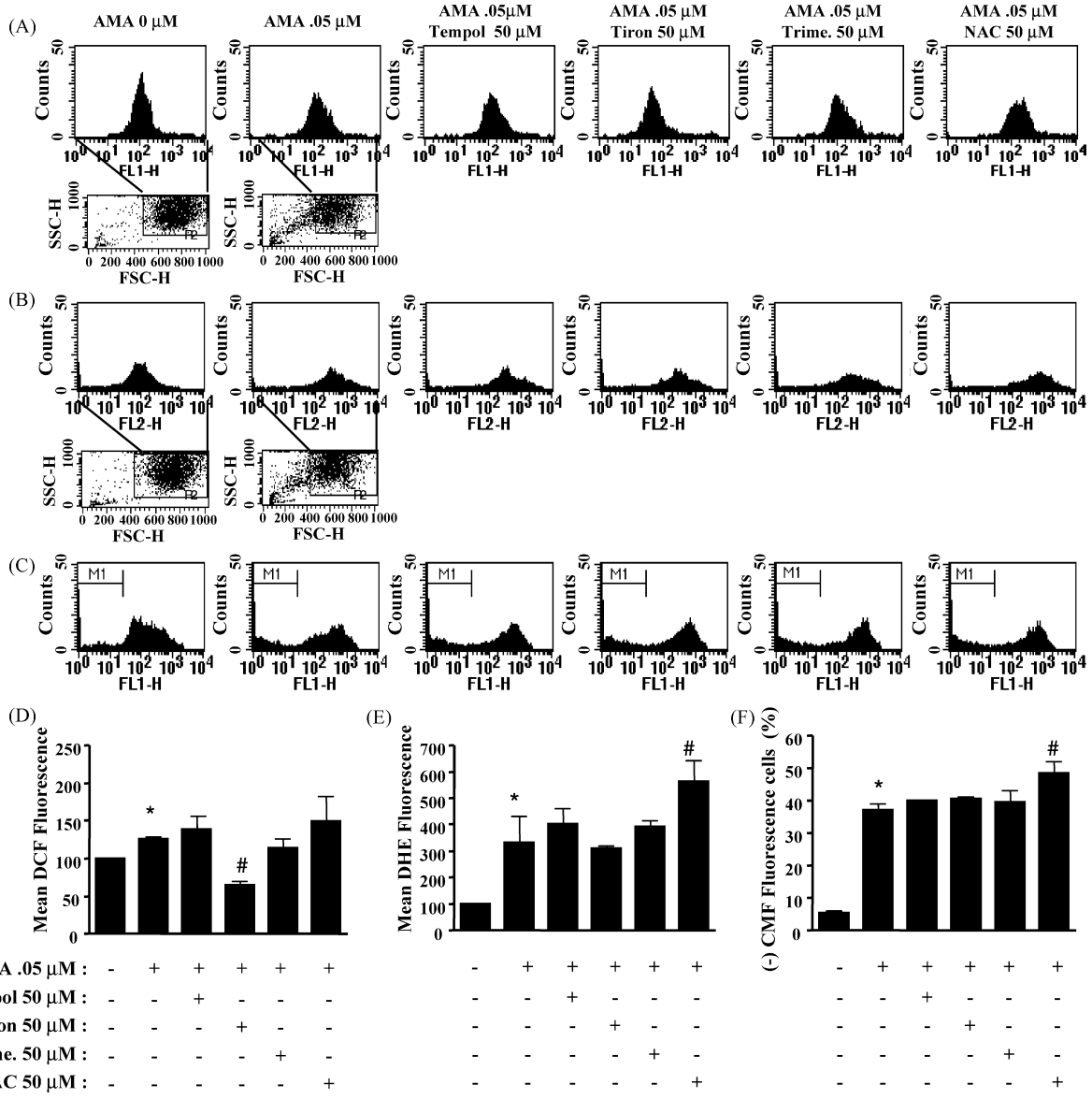

Fig. 4 – Effects of ROS scavengers on intracellular ROS and GSH production in AMA-treated As4.1 cells. Exponentially growing cells were treated with the indicated ROS scavengers in addition to 0.05 μM of AMA for 48 h. (A) Intracellular H_2O_2 level, which is derived from the cells in R2 region of the FSC and SSC dot plot. (B) Intracellular $O_2^{\bullet-}$ level from R2 region. (C) Intracellular GSH level. Graphs show the levels of mean DCF fluorescence of A (D), mean DHE fluorescence of B (E) and mean CMF fluorescence of C (F). $^{*}p < 0.05$ compared with the control group. $^{\#}p < 0.05$ compared with the only AMA-treated cells.

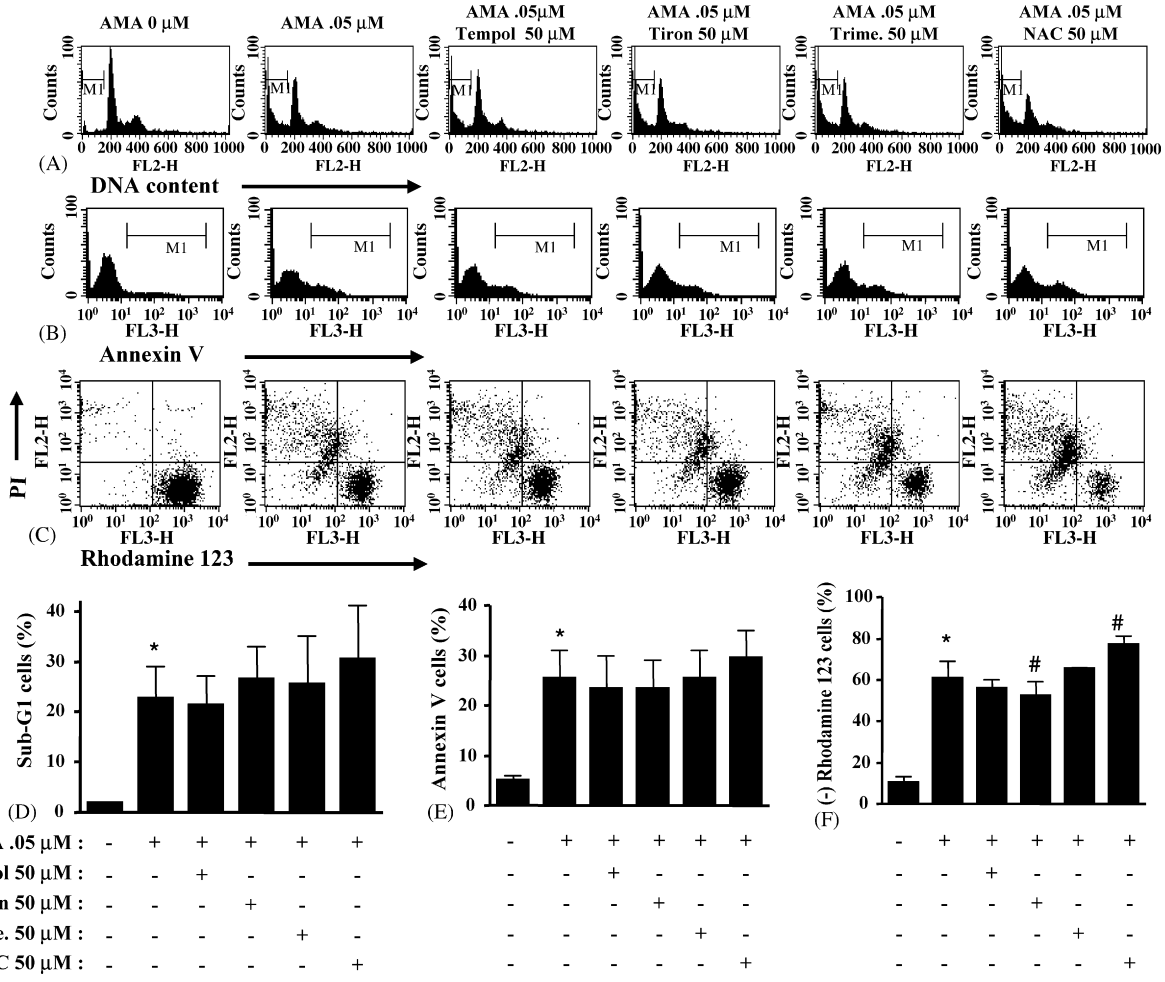

Fig. 5 – Effects of ROS scavengers on AMA-induced apoptosis. Exponentially growing cells were treated with the indicated ROS scavengers in addition to 0.05 μM of AMA for 48 h. (A) Sub-G1 cells, (B) annexin positive cells and (C) Rhodamine 123 negative cells were measured with flow cytometric analysis in Section 2. Graphs show the percentage of sub-G_1 population from A (D), annexin positive cells from B (E) and Rhodamine 123 negative cells from C (F). $^{*}p < 0.05$ compared with the control group. $^{\#}p < 0.05$ compared with the only AMA-treated cells.

not decrease the sub-G1 cell population in AMA-treated As4.1 cells (Fig. 5A and D). However, NAC amplified the sub-G1 cell population. In view of annexin V positive staining, all the scavengers could not decrease the As4.1 cells having annexin V positive stain by AMA. And Tempol could slightly prevent the loss of mitochondrial membrane potential ($\Delta\Psi_m$) and Tiron significantly inhibited the loss of mitochondrial membrane potential ($\Delta\Psi_m$) (Fig. 5C and F). Trimetazidine did not block the loss of mitochondrial membrane potential ($\Delta\Psi_m$). NAC even significantly augmented the loss of mitochondrial membrane potential ($\Delta\Psi_m$) (Fig. 5C and F). Additionally, when we used the higher concentration (0.1, 0.5, 2.5 mM) of ROS scavengers, these concentrations could not significantly changes apoptosis parameters (data not shown). In regard to the cell cycle distribution by AMA and ROS scavengers, AMA did not show any specific phase arrest of cell cycle in As4.1 cells and the scavengers did not significantly alter cell cycle distribution in AMA-treated cells (Fig. 6).

3.3. *Effects of SOD and catalase on ROS production, GSH depletion and apoptosis in AMA-treated As4.1 cells*

Next, to determine whether ROS production and GSH depletion in AMA-treated As4.1 cells were changed by SOD and catalase, As4.1 cells were treated with AMA in the presence or absence of SOD (30 unit/ml) or/and catalase (30 unit/ml) for 48 h. As shown in Fig. 7A and D, SOD and catalase significantly decreased the level of H_2O_2 in AMA-treated As4.1 cells. There was no synergistic or addictive effect of SOD and catalase on reducing the intracellular H_2O_2 in As4.1 cells. In regard to the $O_2^{\bullet-}$ levels by SOD and catalase, SOD and catalase did not decrease the increased $O_2^{\bullet-}$ levels in AMA-treated cells (Fig. 7B and E). When we assessed the level of intracellular GSH in AMA-treated cells in presence of SOD or/and catalase, SOD and catalase did not alter the depletion of GSH content in As4.1 cells treated with AMA.

Next, we examined whether SOD and catalase prevent AMA-induced As4.1 cell death. Co-incubation of SOD and

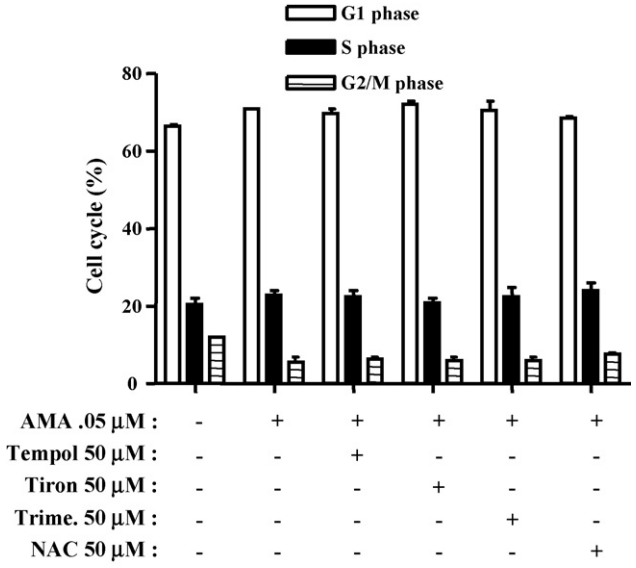

Fig. 6 – Effects of ROS scavengers on cell cycle distribution in AMA-treated As4.1 cells. Exponentially growing cells were treated with the indicated ROS scavengers in addition to 0.05 μM of AMA for 48 h. Graph shows the cell cycle distribution by AMA and ROS scavengers. Results represent the mean of at least two or three independent experiments; bar, S.E.M.

catalase slightly decreased the number of annexin V positive staining in As4.1 cells treated with AMA (Fig. 8A and C). SOD significantly reduced the loss of mitochondrial transmembrane potential ($\Delta\Psi_m$) in AMA-treated As4.1 cells and catalase slightly reduced the loss. Only SOD or/and catalase as a control experiment conserved strongly mitochondrial transmembrane potential ($\Delta\Psi_m$) in As4.1 cells (Fig. 8B and D). In regard to the cell cycle distribution by SOD and catalase, these could not alter cell cycle distribution in AMA-treated cells (Fig. 9). When we used SOD (60 unit/ml) and catalase (60 unit/ml) in this experiment, these concentrations show no differences in ROS production, GSH content, apoptosis parameters and cell cycle distribution in comparison with SOD (30 unit/ml) and catalase (30 unit/ml) (data not shown).

4. Discussion

Since, we have previously shown that AMA induced apoptosis in As4.1 cells via the loss of mitochondrial transmembrane potential ($\Delta\Psi_m$) (now in press). Now we focused on the involvement of ROS, such as H_2O_2 and $O_2^{\bullet-}$ and GSH in the AMA-induced As4.1 cell death and investigated whether ROS scavengers could rescue As4.1 cell death and its mechanism.

Our data showed that the intracellular H_2O_2 and $O_2^{\bullet-}$ levels were significantly increased in AMA-treated As4.1 cells. In fact, 0.05 μM AMA could efficiently induce apoptosis in As4.1 cells. These results are consistent with other reports, showing

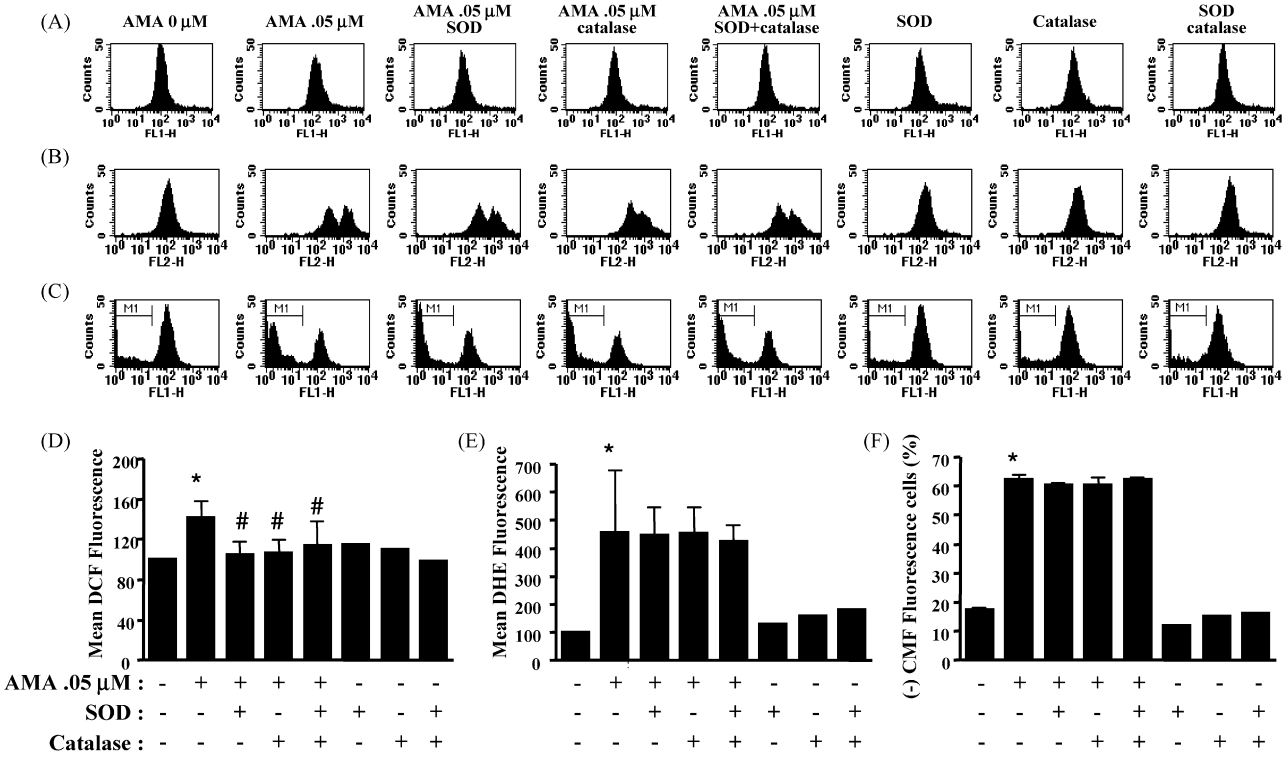

Fig. 7 – Effects of SOD and catalase on intracellular ROS and GSH production in AMA-treated As4.1 cells. Exponentially growing cells were treated with the SOD, catalase and AMA for 48 h. (A) Intracellular H_2O_2 level. (B) Intracellular $O_2^{\bullet-}$ level. (C) Intracellular GSH level. Graphs show the levels of mean DCF fluorescence of A (D), mean DHE fluorescence of B (E) and mean CMF fluorescence of C (F). $^{*}p < 0.05$ compared with the control group. $^{\#}p < 0.05$ compared with the only AMA-treated cells.

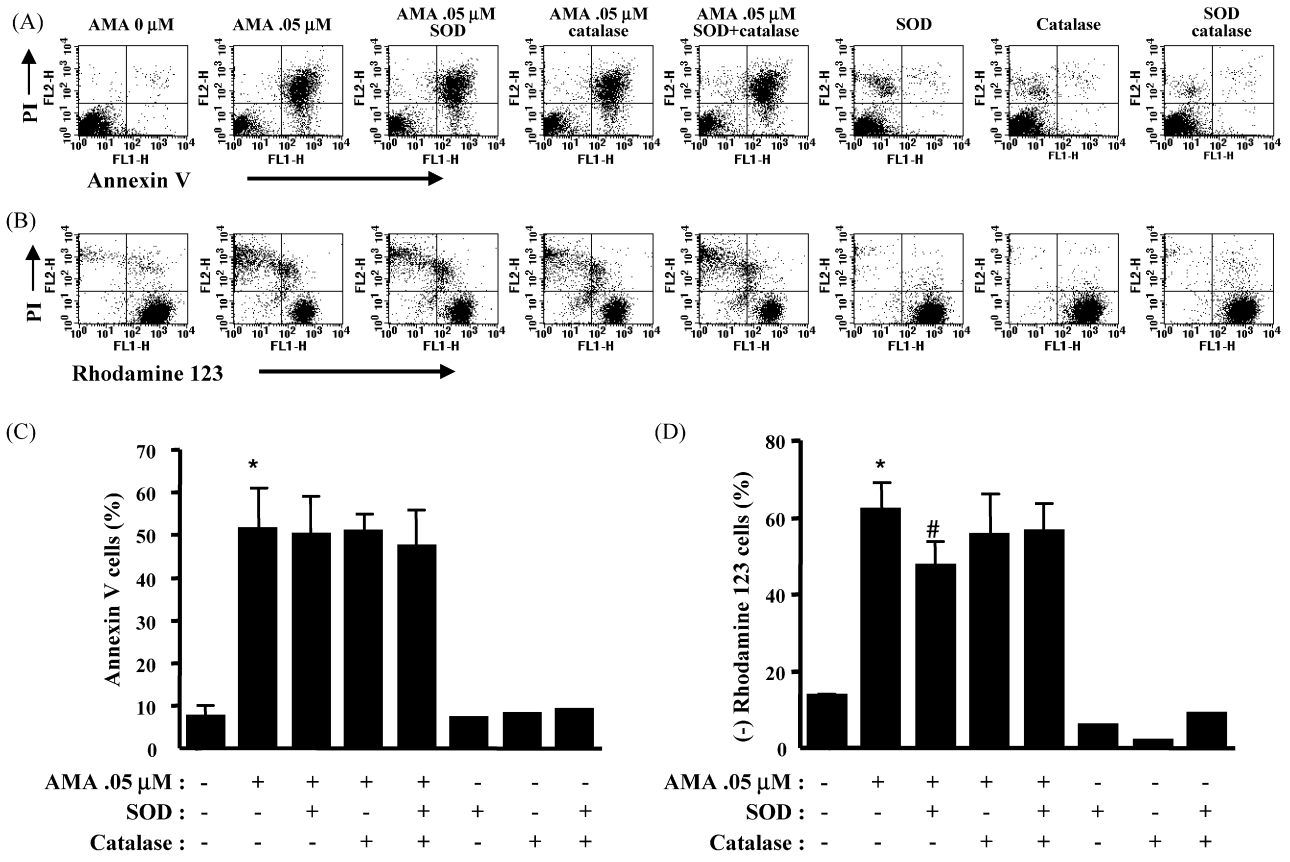

Fig. 8 – Effects of SOD and catalase on AMA-induced apoptosis. Exponentially growing cells were treated with the SOD, catalase and AMA for 48 h. (A) Annexin positive cells and (B) Rhodamine 123 negative cells were measured with flow cytometric analysis in Section 2. Graphs show the percentage of annexin positive cells from A (C) and Rhodamine 123 negative cells from B (D). $^{*}p < 0.05$ compared with the control group. $^{\#}p < 0.05$ compared with the only AMA-treated cells.

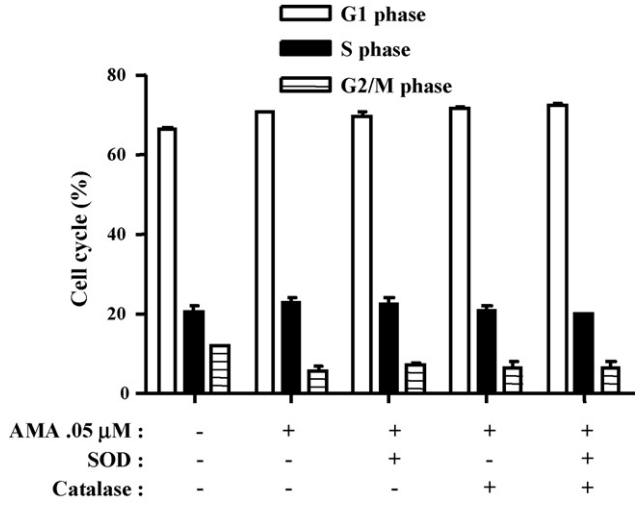

Fig. 9 – Effects of SOD and catalase on cell cycle distribution in AMA-treated As4.1 cells. Exponentially growing cells were treated with the SOD, catalase and AMA for 48 h. Graph shows the cell cycle distribution by SOD, catalase and AMA. Results represent the mean of at least two or three independent experiments; bar, S.E.M.

that increased intracellular H_2O_2 played an important role in AMA-induced cell death in liver cells [37,38] and A549 human lung cancer cells [16]. Also the increased $O_2^{\bullet-}$ levels by AMA was reported in human lung epithelial cells [39]. These findings suggest that the apoptotic effects of AMA are comparative to intracellular ROS level, especially H_2O_2. Interestingly, the intracellular H_2O_2 level was markedly decreased in the short time exposure of AMA and then was increased. This transient decrease is likely to be from the reduced activity of SOD rather than the increased activity of catalase and peroxidase because the level of $O_2^{\bullet-}$ was manifestly increased at the same time.

We tried to know whether the intracellular changes of H_2O_2 and $O_2^{\bullet-}$ levels by ROS scavengers prevent the cell death induced by AMA. Tiron only could significantly reduce the level of H_2O_2 in As4.1 cells treated with AMA. However, this decrease was not in proportion to the decrease level of sub-G1 cells and annexin V staining cells, indicating that the changes of intracellular H_2O_2 by AMA are not directly related to apoptosis in As4.1 cells. Interestingly, Tiron could partially prevent the loss of mitochondrial transmembrane potential ($\Delta\Psi_m$), suggesting that the slight reduced intracellular H_2O_2 level by Tiron plays a role in protection of mitochondrial

transmembrane potential ($\Delta\Psi_m$) rather than in inhibiting of apoptosis resulting from entire cell damage. This notion could be supported by the result that SOD significantly reduced the intracellular H_2O_2 and the loss of mitochondrial transmembrane potential ($\Delta\Psi_m$) without preventing the apoptosis in AMA-treated cells. And catalase showing the significant reduction of intracellular H_2O_2 level slightly inhibited the loss of mitochondrial transmembrane potential ($\Delta\Psi_m$), suggesting that the changes of intracellular H_2O_2 levels in AMA-treated As4.1 cells are important to maintenance of mitochondria membrane potential. It is of note that we could not observe the synergistic or addictive effects of SOD and catalase on the reduction of intracellular H_2O_2 level and of loss of mitochondrial transmembrane potential ($\Delta\Psi_m$). In contrast, catalase even neutralized the ability of SOD to inhibit the loss of mitochondrial transmembrane potential ($\Delta\Psi_m$) in AMA-treated cells. Probably, these results come from different pathways of reducing intracellular H_2O_2 levels by SOD and catalase. In fact, catalase can directly reduce the intracellular H_2O_2 level, however, SOD does not, suggesting that the unidentified mediators activated by SOD are required for reducing the intracellular H_2O_2 levels. These unidentified mediators as well as the lower H_2O_2 levels are likely to be important for recovery of loss of mitochondrial transmembrane potential ($\Delta\Psi_m$) in AMA-treated cells. If catalase could disrupt these unknown mediators activated by SOD, catalase would neutralize the mitochondria protection ability of SOD in AMA-treated cells, resulting in non-synergistic or addictive effects of SOD and catalase. With regard to the $O_2^{\bullet-}$ levels, even Tempol and Tiron as stable SOD mimetics [34,40,41] did not reduce the accumulating of $O_2^{\bullet-}$ level in AMA-treated cells. The inability of Tempol and Tiron as $O_2^{\bullet-}$ scavengers might be due to the peculiarity of As4.1 cells, since we have detected that these scavengers significantly decreased level of $O_2^{\bullet-}$ in AMA-treated Calu-6 lung carcinoma cells and HeLa cervical cancer cell (data not shown). Also, SOD used in our experiment did not reduce the $O_2^{\bullet-}$ level in AMA-treated cells, suggesting that there is the variety of SOD isoforms.

With regard to the intracellular GSH, this is a main non-protein antioxidant in the cell, and it could clear away the superoxide anion free radical and provide electrons for enzymes, such as glutathione peroxidase, which reduce H_2O_2 to H_2O. Our result clearly indicates the depletion of intracellular GSH content by AMA in As4.1 cells. These results support that intracellular GSH levels are inversely comparative to cell death. No effect of ROS scavengers, SOD and catalase on preventing apoptosis in AMA-treated cells was likely to be failure of the recovery of the GSH depletion induced by AMA. Interestingly, NAC showing significantly the augmented GSH depletion and the increased $O_2^{\bullet-}$ level intensified the apoptosis, suggesting that NAC plays a role as an oxidant rather than an anti-oxidant. Recent studies suggest that some substances, such as ascorbic acid and tannic acid that have been regarded as anti-oxidant agents can stimulate the generation of ROS and show pro-oxidant effect under certain circumstance [42,43]. In view of the cell cycle distribution by AMA, ROS scavengers, SOD and catalase, all the agents including the AMA did not induce any specific phase arrest of cell cycle in As4.1 cells, indicating that the changes of ROS level and GSH content are not tightly associated the cell cycle regulation in As4.1 cells.

It has been speculated that the kidney and juxtaglomerular apparatus (JGA) contain an ROS generating system that is responsive to angiotensin II [5,44]. ROS in the JGA-related cells are related to regulation of blood pressure [5,44]. However, the role of ROS in kidney cell death, especially JG cell, has not been evaluated in inspection of apoptosis. Therefore, understanding the molecular mechanism of kidney cell death by ROS generator. such as AMA is an important subject.

In conclusion, we have demonstrated that AMA generates potently ROS, H_2O_2 and $O_2^{\bullet-}$ and induces the depletion of GSH content in As4.1 JG cells, and Tiron, SOD and catalase inhibit to a lesser extent the loss of mitochondrial transmembrane potential ($\Delta\Psi_m$) via the down-regulation of intracellular H_2O_2 level.

Acknowledgements

This research was supported by the Korea Research Foundation Grant funded by the Korean Government (MOEHRD) and the Korean Science and Engineering Foundation (R01-2006-000-10544-0).

REFERENCES

[1] Gonzalez C, Sanz-Alfayate G, Agapito MT, Gomez-Nino A, Rocher A, Obeso A. Significance of ROS in oxygen sensing in cell systems with sensitivity to physiological hypoxia. Respir Physiol Neurobiol 2002;132:17–41.
[2] Baran CP, Zeigler MM, Tridandapani S, Marsh CB. The role of ROS and RNS in regulating life and death of blood monocytes. Curr Pharm Des 2004;10:855–66.
[3] Bubici C, Papa S, Pham CG, Zazzeroni F, Franzoso G. The NF-kappaB-mediated control of ROS and JNK signaling. Histol Histopathol 2006;21:69–80.
[4] Zorov DB, Juhaszova M, Sollott SJ. Mitochondrial ROS-induced ROS release: an update and review. Biochim Biophys Acta 2006;1757:509–17.
[5] Wilcox CS. Reactive oxygen species: roles in blood pressure and kidney function. Curr Hypertension Rep 2002;4:160–6.
[6] Chen TJ, Jeng JY, Lin CW, Wu CY, Chen YC. Quercetin inhibition of ROS-dependent and -independent apoptosis in rat glioma C6 cells. Toxicology 2006;223:113–26.
[7] Dasmahapatra G, Rahmani M, Dent P, Grant S. The tyrphostin adaphostin interacts synergistically with proteasome inhibitors to induce apoptosis in human leukemia cells through a reactive oxygen species (ROS)-dependent mechanism. Blood 2006;107:232–40.
[8] Wallach-Dayan SB, Izbicki G, Cohen PY, Gerstl-Golan R, Fine A, Breuer R. Bleomycin initiates apoptosis of lung epithelial cells by ROS but not by Fas/FasL pathway. Am J Physiol 2006;290:L790–6.
[9] Simon HU, Haj-Yehia A, Levi-Schaffer F. Role of reactive oxygen species (ROS) in apoptosis induction. Apoptosis 2000;5:415–8.
[10] Nakayama K, Okamoto F, Harada Y. Antimycin A: isolation from a new Streptomyces and activity against rice plant blast fungi. J Antibiotics 1956;9:63–6.
[11] Campo ML, Kinnally KW, Tedeschi H. The effect of antimycin A on mouse liver inner mitochondrial membrane channel activity. J Biol Chem 1992;267:8123–7.

[12] Maguire JJ, Kagan VE, Packer L. Electron transport between cytochrome c and alpha tocopherol. Biochem Biophys Res Commun 1992;188:190–7.
[13] Pham NA, Robinson BH, Hedley DW. Simultaneous detection of mitochondrial respiratory chain activity and reactive oxygen in digitonin-permeabilized cells using flow cytometry. Cytometry 2000;41:245–51.
[14] Alexandre A, Lehninger AL. Bypasses of the antimycin a block of mitochondrial electron transport in relation to ubisemiquinone function. Biochim Biophys Acta 1984;767:120–9.
[15] Balaban RS, Nemoto S, Finkel T. Mitochondria, oxidants, and aging. Cell 2005;120:483–95.
[16] Panduri V, Weitzman SA, Chandel NS, Kamp DW. Mitochondrial-derived free radicals mediate asbestos-induced alveolar epithelial cell apoptosis. Am J Physiol 2004;286:L1220–7.
[17] Petronilli V, Penzo D, Scorrano L, Bernardi P, Di Lisa F. The mitochondrial permeability transition, release of cytochrome c and cell death. Correlation with the duration of pore openings in situ. J Biol Chem 2001;276:12030–4.
[18] Costantini P, Chernyak BV, Petronilli V, Bernardi P. Modulation of the mitochondrial permeability transition pore by pyridine nucleotides and dithiol oxidation at two separate sites. J Biol Chem 1996;271:6746–51.
[19] Pastorino JG, Tafani M, Rothman RJ, Marcinkeviciute A, Hoek JB, Farber JL. Functional consequences of the sustained or transient activation by Bax of the mitochondrial permeability transition pore. J Biol Chem 1999;274:31734–9.
[20] King MA. Antimycin A-induced killing of HL-60 cells: apoptosis initiated from within mitochondria does not necessarily proceed via caspase 9. Cytometry A 2005;63:69–76.
[21] Wolvetang EJ, Johnson KL, Krauer K, Ralph SJ, Linnane AW. Mitochondrial respiratory chain inhibitors induce apoptosis. FEBS Lett 1994;339:40–4.
[22] Kaushal GP, Ueda N, Shah SV. Role of caspases (ICE/CED 3 proteases) in DNA damage and cell death in response to a mitochondrial inhibitor, antimycin A. Kidney Int 1997;52:438–45.
[23] de Graaf AO, Meijerink JP, van den Heuvel LP, DeAbreu RA, de Witte T, Jansen JH, et al. Bcl-2 protects against apoptosis induced by antimycin A and bongkrekic acid without restoring cellular ATP levels. Biochim Biophys Acta 2002;1554:57–65.
[24] Robertson PW, Klidjian A, Harding LK, Walters G, Lee MR, Robb-Smith AH. Hypertension due to a renin-secreting renal tumour. Am J Med 1967;43:963–76.
[25] Kihara I, Kitamura S, Hoshino T, Seida H, Watanabe T. A hitherto unreported vascular tumor of the kidney: a proposal of ''juxtaglomerular cell tumor''. Acta Pathol Japonica 1968;18:197–206.
[26] Duan X, Bruneval P, Hammadeh R, Fresco R, Eble JN, Clark JI, et al. Metastatic juxtaglomerular cell tumor in a 52-year-old man. Am J Surg Pathol 2004;28:1098–102.
[27] Sigmund CD, Okuyama K, Ingelfinger J, Jones CA, Mullins JJ, Kane C, et al. Isolation and characterization of renin-expressing cell lines from transgenic mice containing a renin-promoter viral oncogene fusion construct. J Biol Chem 1990;265:19916–22.
[28] Park WH, Jung CW, Park JO, Kim K, Kim WS, Im YH, et al. Trichostatin inhibits the growth of ACHN renal cell carcinoma cells via cell cycle arrest in association with p27, or apoptosis. Int J Oncol 2003;22:1129–34.
[29] Poot M, Kavanagh TJ, Kang HC, Haugland RP, Rabinovitch PS. Flow cytometric analysis of cell cycle-dependent changes in cell thiol level by combining a new laser dye with Hoechst 33342. Cytometry 1991;12:184–7.
[30] Macho A, Hirsch T, Marzo I, Marchetti P, Dallaporta B, Susin SA, et al. Glutathione depletion is an early and calcium elevation is a late event of thymocyte apoptosis. J Immunol 1997;158:4612–9.
[31] Hedley DW, Chow S. Evaluation of methods for measuring cellular glutathione content using flow cytometry. Cytometry 1994;15:349–58.
[32] Poot M, Teubert H, Rabinovitch PS, Kavanagh TJ. De novo synthesis of glutathione is required for both entry into and progression through the cell cycle. J Cell Physiol 1995;163:555–60.
[33] Schnelldorfer T, Gansauge S, Gansauge F, Schlosser S, Beger HG, Nussler AK. Glutathione depletion causes cell growth inhibition and enhanced apoptosis in pancreatic cancer cells. Cancer 2000;89:1440–7.
[34] Yamada J, Yoshimura S, Yamakawa H, Sawada M, Nakagawa M, Hara S, et al. Cell permeable ROS scavengers, Tiron and Tempol, rescue PC12 cell death caused by pyrogallol or hypoxia/reoxygenation. Neurosci Res 2003;45:1–8.
[35] Tikhaze AK, Lankin VZ, Zharova EA, Kolycheva SV. Trimetazidine as indirect antioxidant. Bull Exp Biol Med 2000;130:951–3.
[36] Stanley WC, Marzilli M. Metabolic therapy in the treatment of ischaemic heart disease: the pharmacology of trimetazidine. Fund Clin Pharmacol 2003;17:133–45.
[37] Chen HM, Ma HH, Yan XJ. Inhibitory effect of agarohexaose on antimycin A induced generation of reactive oxygen species. Acta Pharm Sin (Yao xue xue bao) 2005;40:903–7.
[38] Chen HM, Yan XJ. Antioxidant activities of agaro-oligosaccharides with different degrees of polymerization in cell-based system. Biochim Biophys Acta 2005;1722:103–11.
[39] Li C, Wright MM, Jackson RM. Reactive species mediated injury of human lung epithelial cells after hypoxia-reoxygenation. Exp Lung Res 2002;28:373–89.
[40] Cuzzocrea S, McDonald MC, Mazzon E, Siriwardena D, Costantino G, Fulia F, et al. Effects of tempol, a membrane-permeable radical scavenger, in a gerbil model of brain injury. Brain Res 2000;875:96–106.
[41] Greenstock CL, Miller RW. The oxidation of tiron by superoxide anion. Kinetics of the reaction in aqueous solution in chloroplasts. Biochim Biophys Acta 1975;396:11–6.
[42] Li JJ, Tang Q, Li Y, Hu BR, Ming ZY, Fu Q, et al. Role of oxidative stress in the apoptosis of hepatocellular carcinoma induced by combination of arsenic trioxide and ascorbic acid. Acta Pharmacol Sin 2006;27:1078–84.
[43] Khan NS, Ahmad A, Hadi SM. Anti-oxidant, pro-oxidant properties of tannic acid and its binding to DNA. Chemico-Biol Interact 2000;125:177–89.
[44] Wilcox CS. Redox regulation of the afferent arteriole and tubuloglomerular feedback. Acta Physiol Scand 2003;179:217–23.